

# Intramolecular Rearrangement of Six-Coordinate Structures

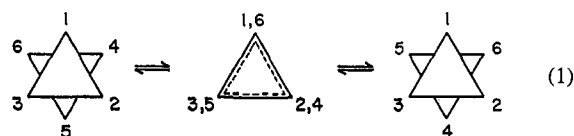
E. L. Muetterties

Contribution from Frick Chemical Laboratory, Princeton University, Princeton, New Jersey 08540, and (No. 1422) Central Research Department, Experimental Station, E. I. du Pont de Nemours and Company, Wilmington, Delaware 19898. Received February 14, 1968

**Abstract:** Possible labile six-coordinate structures are discussed in the context of intramolecular rearrangement via "twisting" mechanisms. The stereochemical rigidity of six-coordinate complexes, although intrinsically greater than that of five- or seven-coordinate species, should not be inordinately great. Topological delineation of octahedral rearrangements through trigonal prismatic intermediates or transition states is presented for the  $ML_6$ ,  $M(\text{chel})_3$ ,  $M(\text{unsym-chel})_3$ ,  $M(\text{chel})_2XY$ , and  $M(\text{unsym-chel})(\text{unsym-chel}')(\text{unsym-chel}'')$  octahedral classes.

Octahedral or near-octahedral geometry overwhelmingly prevails for six-coordinate species. An alternative constitutional isomer, the trigonal prism, is unknown for *discrete*  $ML_6$  molecules or ions although there is one class of metal chelates  $M(S_2C_2R_2)_3$  (*vide infra*) of  $D_{3h}$  symmetry. With this one class exception, it appears that the potential energy surface of a *discrete* six-coordinate complex will show a significant minimum at octahedral-molecular parameters and that there may or may not be a minimum at the shape parameters corresponding to a trigonal prism. For most six-coordinate complexes, the energy difference between the octahedron and the trigonal prism must be relatively large. The relative qualification refers to packing effects in the solid state, stereospecific solvation in solution, or steric and electronic variations in the ligand. If this were not a realistic assessment, then there would be many more examples of discrete trigonal prismatic structures, particularly for the solid state. Trigonal prismatic  $S_6$  coordination arrays are commonly found in inorganic sulfides  $MoS_2$ ,<sup>1</sup>  $TiS$ ,<sup>1</sup>  $Hf_2S$ ,<sup>2</sup> and  $VS_{1-2}$ ,<sup>2,3</sup> but the significance of this geometry found in nonmolecular sulfide lattices is difficult to assess realistically for relevance to the geometry question for discrete six-coordinate complexes.

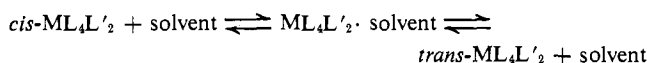
The barrier to polyhedral rearrangement from octahedral to trigonal prismatic also appears to be generally large, at least compared with the stereochemically nonrigid five-coordinate polyhedra.<sup>4-9</sup> Isomerization and racemization of octahedral structures are well documented in the literature. Inferentially, most of these rearrangements appear to proceed primarily by dissociation rather than through a trigonal prismatic intermediate or transition state. However, a more precise characterization of these isomerization studies is that none has unequivocally established the face-rotation mechanism (eq 1) and other alternative twist processes



(*vide infra*). In most reported studies, there is no operational distinction between dissociative and intramolecular mechanisms, *i.e.*, there is no physical probe extant that would provide identification of the trigonal rotation route for the six-coordinate complexes. A *dominant* dissociative isomerization mechanism could be defined, for example, in a *cis*- $MCl_4F_2$  complex if  $F^{19}$  nmr spectra showed M-F bond breaking to be of comparable rate to *cis-trans* isomerization. Such experiments would not rule out intramolecular rearrangement as a contributing mechanism for isomerization but would show that alternative isomerization paths are of higher energy. Operational definition (nmr) of a nonbond-breaking mechanism could be visualized for a molecule such as the hypothetical *cis*- $PtF_4(PR_3)_2$  if isomerization were fast on the nmr time scale at say  $100^\circ$ ,  $F^{19}$ -Pt and  $P^{31}$ -Pt coupling were retained above this temperature, and the intramolecular label were satisfied by appropriate concentration studies.<sup>10</sup> This hypothetical experiment would not exclude the possibility of dissociation as a slower isomerization pathway; the experiment simply would identify the nonbond-breaking<sup>11</sup> mechanism as the lowest energy isomerization mechanism.

Metal chelates present a more difficult system for operational delineation of a nonbond-breaking isomerization mechanism. Consider the system analyzed by Faller and Davison.<sup>12</sup> The  $25^\circ$  proton nmr spectrum of  $(\text{acac})_2\text{SnCl}_2$  is consistent only with *cis*-octahedral geometry. There are two distinct  $CH_3$  resonances and satellites due to spin-spin coupling between  $H_{CH,CH_3}$  and  $Sn^{117,119}$  nuclei. At elevated temperatures, the spectrum undergoes changes analyzable as an exchange of proton ( $CH_3$ ) nuclear positions. At  $140^\circ$ , there are single CH and single  $CH_3$  resonances with retention of Sn-H coupling. Dissociative mechanisms including

(10) The experiment would necessarily be effected in an inert solvent to preclude the possibility of an associative isomerization process of the type



(11) Nmr definition: metal atom-ligand atom coupling preserved.  
(12) J. W. Faller and A. Davison, *Inorg. Chem.*, **6**, 182 (1967).

(1) A. F. Wells, "Structural Inorganic Chemistry," Oxford Press, Clarendon, 1962, p 520.

(2) H. F. Franzen, *J. Inorg. Nucl. Chem.*, **28**, 1575 (1966).

(3) H. F. Franzen and S. Westman, *Acta Chem. Scand.*, **17**, 2353 (1963).

(4) S. Berry, *J. Chem. Phys.*, **32**, 933 (1960).

(5) (a) E. L. Muetterties, *Inorg. Chem.*, **4**, 769 (1965); (b) *ibid.*, **6**, 635 (1967).

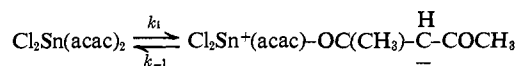
(6) E. L. Muetterties, W. Mahler, and R. Schmutzler, *ibid.*, **2**, 213 (1963).

(7) E. L. Muetterties, W. Mahler, K. J. Packer, and R. Schmutzler, *ibid.*, **3**, 1298 (1964).

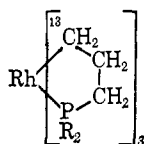
(8) E. L. Muetterties and W. Mahler, *ibid.*, **4**, 1520 (1965).

(9) E. L. Muetterties and R. A. Schunn, *Quart. Rev. (London)*, **20**, 245 (1966).

Sn-Cl bond breaking cannot be eliminated as possibilities. Furthermore, single Sn-O bond breaking may be fast even though Sn-H coupling is retained at elevated temperatures because one end of the chelate could still be bound to the metal atom. The thermodynamic equilibrium

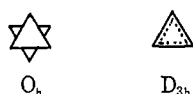


could lie far to either side. With  $k$  comparable to the nmr time scale, such a mechanism would be consistent with the experimental data. Considering the physical probes available today, *there can be no experimental definition of a "nonbond-breaking" permutation of nuclear positions for isomerization of chelates* of the type  $\text{M}(\text{unsym-chel})_3$  or  $\text{M}(\text{chel})_2\text{X}_2$  unless (1) all the ligand atoms directly bound to the metal have magnetic moments, (2) the metal atom is subject to an nmr experiment, and (3) complete fine structure, expected from the six ligand nuclei bound to the metal atom, is present in the metal nmr resonance at some temperature below and some temperature above that where isomerization is fast on the nmr time scale. A purely hypothetical system comprises *cis* and *trans*



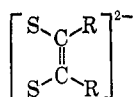
where  $I$  is  $1/2$  for the  $^{103}\text{Rh}$ ,  $^{31}\text{P}$ , and  $^{13}\text{C}$  nuclei.

**Trigonal Prismatic Complexes.** Symmetry considerations alone do not characterize the trigonal prism as an unfavorable six-coordinate geometry. Clearly, however, intramolecular ligand atom interactions are maximized in  $D_{3h}$  as illustrated in views down the  $C_3$  axes of the trigonal prism and the octahedron.



If the ligand atoms have all energetically available orbitals filled, then the ligand atom-ligand atom interactions are nonbonding and repulsive and the octahedral geometry should be more stable than trigonal prismatic. One of the earlier, approximate valence-bond comparisons of the octahedron and trigonal prism was by Hultgren,<sup>13</sup> who concluded that the trigonal prism achieves greater resonance energy per bond than the octahedron but that this is more than offset by the ligand atom-ligand atom repulsion in the former. Hultgren also proposed that the trigonal prism would become more favorable as (1) the MX bonds become less ionic, (2) the ligand atoms decrease in size, and (3) the relative energy level of the d orbitals falls.

The only *discrete*, trigonal prismatic complexes known today are based on the dithiolate ligand



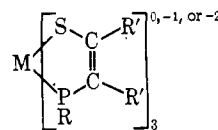
and the neutral complexes with geometry rigorously

(13) R. Hultgren, *Phys. Rev.*, **40**, 891 (1932).

established are  $\text{Re}[\text{S}_2\text{C}_2(\text{C}_6\text{H}_5)_2]_3$ ,<sup>14</sup>  $\text{V}[\text{S}_2\text{C}_2(\text{C}_6\text{H}_5)_2]_3$ ,<sup>15</sup> and  $\text{Mo}(\text{S}_2\text{C}_2\text{H}_2)_3$ .<sup>16</sup> In the rhenium complex, the sulfur atoms quite precisely define a trigonal prism with square faces. The average intra- and interligand S-S separations are 3.04 and 3.05 Å. Similar geometries are found in the other two dithiolates. The S-S interligand separations are strikingly similar: 3.05 Å in  $\text{Re}[\text{S}_2\text{C}_2(\text{C}_6\text{H}_5)_2]_3$ , 3.064 Å in  $\text{V}[\text{S}_2\text{C}_2(\text{C}_6\text{H}_5)_2]_3$ , and 3.11 Å in  $\text{Mo}(\text{S}_2\text{C}_2\text{H}_2)_3$ . It has been suggested that the short S-S separations may be indicative of S-S bonding, which bonding could be the genesis of trigonal-prismatic-geometry stabilization relative to octahedral.

As tentatively proposed,<sup>14</sup> the more reduced or negatively charged trisdithiolate complexes are not trigonal prismatic. In the tetramethylammonium salt of  $\text{V}[\text{S}_2\text{C}_2(\text{CN})_2]_3^{2-}$ , the sulfur atoms define a polyhedron intermediate between the idealized octahedron and trigonal prism.<sup>17</sup> Recently, X-ray studies have shown  $\text{Fe}[\text{S}_2\text{C}_2(\text{CN})_2]_3^{2-}$  in the tetraphenylarsonium salt to be an octahedral complex.<sup>18</sup> High charge density in the ligand sphere appears to swing the pendulum back in favor of the octahedron presumably because of increased coulombic repulsion of sulfur atoms.

Irrespective of the proper theoretical explanation of ground-state geometries of trisdithiolate complexes, the structural and chemical studies clearly establish an important point. In this class of compounds, there is the possibility of very small energy differentiation between the two idealized geometries and of stereochemical lability through facile geometrical interconversions. Such chemistry might be extended to phosphorus which should be electronically similar to sulfur. Then there would be not only the possibility of facile interconversions of idealized geometries but also of an experimental definition (nmr) of intramolecular-face rotation isomerization as in the hypothetical system *cis* and *trans*



**Topological Representation of Stereoisomers and Isomerization in Octahedral Species.** Isomerically, the most complicated six-coordinate system comprises  $\text{ML}_6$  complexes in which all ligand atoms are nuclearly distinguishable. For initial simplicity, consider an  $\text{MX}_6$  molecule in which X atoms are nuclearly identical but assume that each X atom can be labeled (1 through 6) and distinguished. For this general case, there are 30 ( $6!/4 \times 3 \times 2$ ) octahedral isomers and 120 ( $6!/3 \times 2$ ) trigonal prismatic isomers. This system is stereoisomerically "closed." The 30 equivalent (but distinguishable by labels) octahedral isomers can be represented by the edge midpoints of the regular pentagonal dodecahedron<sup>19</sup> in double group form (see Figure

(14) R. Eisenberg and J. A. Ibers, *J. Am. Chem. Soc.*, **87**, 3776 (1965); *Inorg. Chem.*, **5**, 411 (1966).

(15) R. Eisenberg, E. I. Stiefel, R. C. Rosenberg, and H. B. Gray, *J. Am. Chem. Soc.*, **88**, 2874 (1966).

(16) A. E. Smith, G. N. Schrauzer, V. P. Mayweg, and W. Heinrich, *ibid.*, **87**, 5798 (1965).

(17) E. I. Stiefel, Z. Dori, and H. B. Gray, *ibid.*, **89**, 3354 (1967).

(18) I. Bernal and A. Sequeira, paper presented before the American Crystallographers Association, Minneapolis, Minn., Aug 1967.

(19) (a) This polyhedron may be used also for the five-coordinate system with polyhedral vertices and edge midpoints respectively represent-

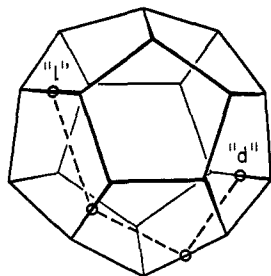
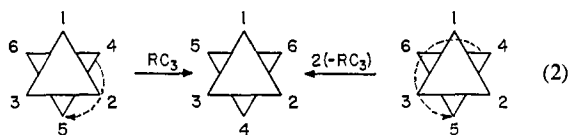


Figure 1. Topological representation of six-coordinate complexes in which all ligand atoms can be distinguished. The 30 octahedral isomers are situated at the midpoints of the edges. The enantiomeric pairs lie on edge midpoints connected by a twofold axis. The minimum number of steps for interconversion of enantiomers is three, as noted by the dotted lines. The trigonal prismatic intermediates are located on the pentagonal faces (see Figure 2). This representation must be in double group form or imaginary solutions result.

1). Enantiomers lie on opposite edge midpoints connected by a twofold axis of symmetry. Restricting the intramolecular isomerization mechanism to rotation ( $RC_3$ )<sup>20</sup> of triangular faces in the octahedron as noted in eq 1, then isomerization paths are defined by the 120 lines (*vide infra*) connecting adjacent and nonadjacent edge midpoints in each pentagonal face. The eight different octahedral isomers generated in one step from a given isomer  $RC_3$  operation are depicted in the dodecahedral fragment shown in Figure 2. Note that the a to c single step consists of  $RC_3$  clockwise rotation equivalent to two counterclockwise rotations  $a \rightarrow b \rightarrow c$  (eq 2).



This isomer "subcycle" of three is one of three subcycle requirements here. The midpoints ( $RC_6$ ) of the dotted lines (or arcs) connecting polyhedral edge midpoints represent the 120 trigonal prismatic species.

The above polyhedral representation may serve as an energy surface for an  $MX_6$  molecule since all edge midpoints are equivalent. It is incomplete except in double group form because there are imaginary pathways.  $RC_3$  operations analogous to the  $RC_3$  operations<sup>20</sup> (difficult to depict but intuitively appealing) yield real pathways, generate the two "isomer" subcycles of four not available in the simple polyhedron, and provide the proper number of minimal racemization pathways. Explicit solutions in multispace are being sought—the 600-cell regular polytope ( $n = 4$ ) is a possibility.

Returning to Figure 1, the reader may easily see the many different possible sequences for conversion of an optically active isomer into its enantiomorph. The minimum number of operations ( $RC_3$ ) required for the enantiomer traverse is three as depicted by dotted lines

ing the 20 trigonal bipyramid and 30 square-pyramid species.<sup>ab</sup> Double group form is required to satisfy pathways, the 12-fold degenerate enantiomer traverse, and the isomer "subcycle" of six ( $RC_3$  operations may produce pseudo-hexagonal faces). (b) The numbering convention is that outlined by E. L. Muetterties and C. M. Wright, *Quart. Rev. (London)*, **21**, 109 (1967).

(20) This  $ML_6$  system is explicitly covered by the molecular point group  $O_h$  or the  $O_h$  double group and symmetry operation 1 is denoted by  $RC_3$ .

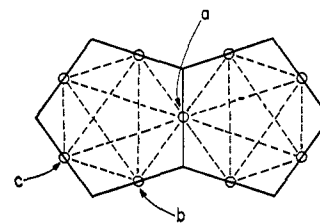
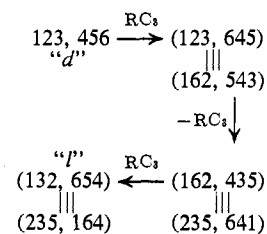


Figure 2. Fragment of the pentagonal dodecahedron. The dotted lines on the pentagonal faces represent isomerization paths with trigonal prismatic intermediates. Each face has ten different trigonal prismatic stereoisomers. " $RC_3$  operations" to exchange a, b, and c positions are required to generate all 24 minimum racemization paths.

in Figure 1. The minimal sequence is  $+ - +$  (or  $- + -$ ) as in

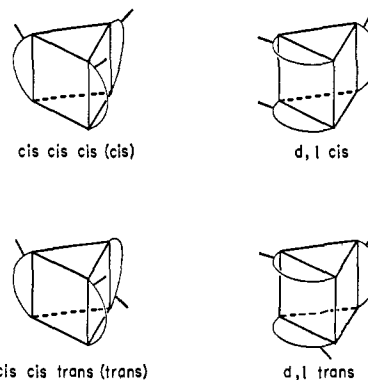


and has a 24-fold degeneracy.

In a six-coordinate molecule or ion in which all ligand atoms are nonequivalent, the pentagonal dodecahedron in double group form (Figures 1 and 2) still provides a topological representation. However, the operations involve imaginary threefold axes ( $iRC_3$ ), and the regular polyhedron is no longer an energy surface. A potential energy surface can be generated from the pentagonal dodecahedron by increasing or decreasing the distance  $r$  to edge midpoint pairs to a degree representative of the energy level differentiation among diastereomers. In the real case of an  $ML_1L_2L_3L_4L_5L_6$  molecule, the minimum steps ( $iRC_3$ ) for  $d$  to  $l$  conversion are still three but the kinetically favored path may comprise more than three  $iRC_3$  operations.

For metal complexes with bidentate ligands, the number of permissible  $RC_3$  rotations is limited because of the constraints of the bridging entity. No trigonal prismatic intermediate can be bridged diagonally across a square face.

For an  $M(\text{unsym-chel})_3$  molecule or ion, there are four octahedral species:  $d, l$  *cis cis cis* ( $a, l$  *cis*) and  $d, l$  *cis cis trans* ( $d, l$  *trans*) and six trigonal prismatic species.



This system may be topologically described by a tetrahedron with vertices representing octahedral isomers

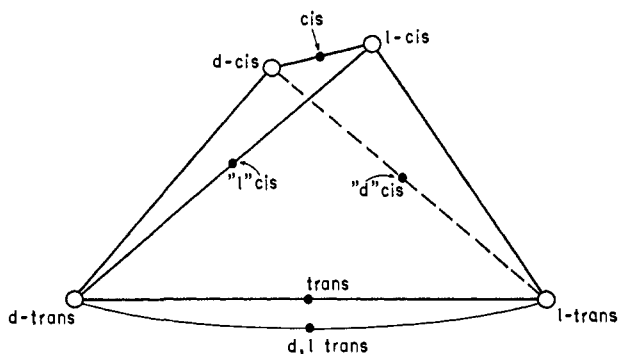


Figure 3. Topological representation of the six-coordinate tris chelate where the chelate ligands are unsymmetrical. Octahedral isomers are at the vertices of the  $C_{2v}$  tetrahedron and trigonal prismatic intermediates are along the edges of the polyhedron. In this system only two kinds of process are possible through  $iRC_3$  operations, namely, inversion and isomerization with inversion of configuration.

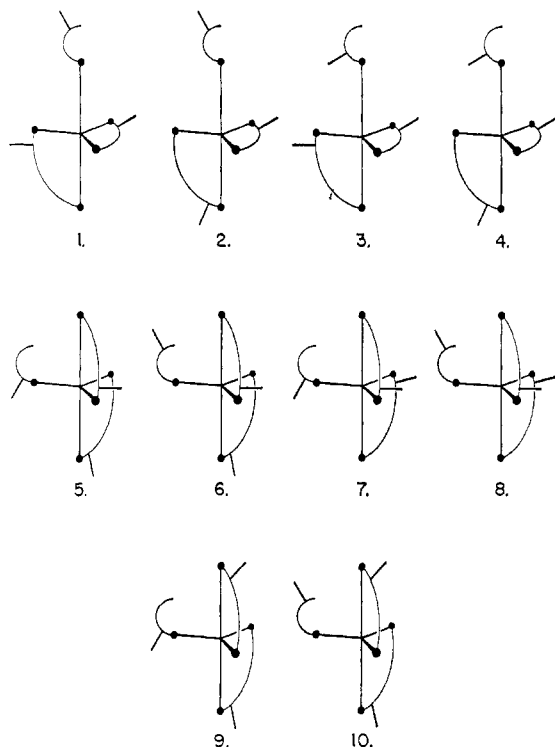


Figure 4. The "d" forms of the ten dissymmetric isomers for a trigonal bipyramidal intermediate in a dissociative isomerization of an  $M(\text{unsym-chel})_3$  species.

with the connecting lines shown in Figure 3 representing  $iRC_3$  operations with trigonal prismatic intermediates or transition states. Note that isomerization occurs only with inversion of configuration. The paths marked *cis* and *trans* involve a Bailar Twist<sup>21</sup> intermediate and the *d* or *l cis* or *trans* paths a Ráy and Dutt Twist<sup>22</sup> intermediate. These paths unless accidentally degenerate are not equivalent—only vertices or dotted line midpoints which represent enantiomers are energetically equivalent. Thus the symmetry of the tetrahedron of Figure 3 is not  $T_d$  but  $C_{2v}$ . Differentiation

(21) J. C. Bailar, Jr., *J. Inorg. Nucl. Chem.*, **8**, 165 (1958). Proposed independently by W. G. Gehman, Ph.D. Thesis, Pennsylvania State University 1954, and L. Seiden, Ph.D. Thesis, Northwestern University 1957. The generic term for an  $RC_3$  or  $iRC_3$  operation is the "Bailar Twist."

(22) P. Ráy and N. K. Dutt, *J. Indian Chem. Soc.*, **20**, 81 (1943).

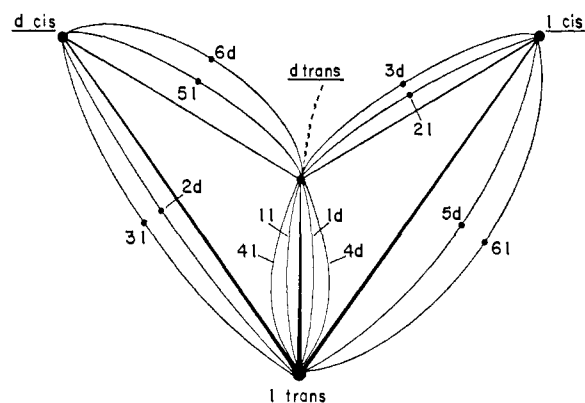
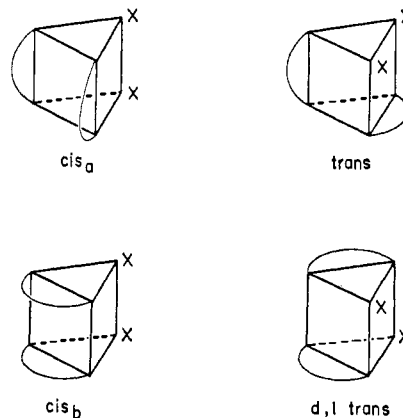


Figure 5. Topological representation of isomerization interrelationships for an  $M(\text{unsym-chel})_3$  species through a trigonal bipyramidal transition state. The octahedral isomers are at the vertices of an open tetrahedron which has no plane or axis of symmetry. The trigonal bipyramidal states are located along the edges of the open tetrahedron. Racemization of the *cis* isomer cannot occur directly and this accounts for the "open" tetrahedron. Isomerization may occur with retention or inversion of configuration. Note that the transition states 7 through 10 (Figure 4) are inactive for both isomerization and racemization.

of energetics for the various pathways will depend upon many factors, perhaps most importantly on Mchel ring flexibility and steric factors as noted by Fay and Piper<sup>23</sup> and by Springer and Sievers.<sup>24</sup>

An alternative rearrangement path may also be topologically described. For example, an  $M(\text{unsym-chel})_3$  complex may rearrange dissociatively through a five-coordinate transition state or intermediate. Assuming trigonal bipyramidal geometry,<sup>25</sup> there are ten dissymmetric diastereomers (Figure 4) for the intermediate state. Topologically this isomerization is depicted in Figure 5 by a dissymmetric set of triangles joined at edges. A distinctive feature is the absence of a one-step racemization for *cis*-octahedral isomers. On the other hand, isomerization may occur with inversion or retention of configuration.

Other chelate systems may be easily described in a topological fashion. The  $M(\text{sym-chel})_3$  case is trivial; the  $M(\text{chel})_2X_2$  (or  $M(\text{chel})_2XY$ ) case is depicted in Figure 6 where the five intermediate trigonal isomers<sup>26</sup> are



(23) R. C. Fay and T. S. Piper, *Inorg. Chem.*, **3**, 348 (1964).

(24) Cf. C. S. Springer, Jr., and R. E. Sievers, *ibid.*, **6**, 852 (1967).

(25) Further assuming a low rate for rearrangement of trigonal bipyramidal to square-pyramidal geometry.

(26) In all trigonal isomers square faces are ideally assumed. For chelate structures, the  $M(\text{chel})$  ring is considered coplanar to simplify conformational problems.

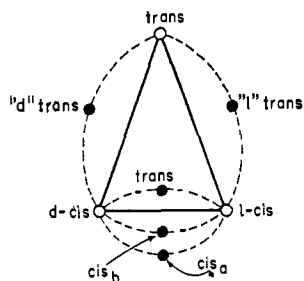


Figure 6. Topological representation of the six-coordinate  $M(\text{chel})_2X_2$  or  $M(\text{chel})_2XY$  system with the octahedral stereoisomers at the vertices of the isosceles triangle. Trigonal prismatic intermediates are along the edges of the triangle.

For the general rearrangement case of octahedral chelates where all chelate ligands are different and unsymmetric,<sup>27</sup> there are 16 isomeric octahedra. Restricting the reaction coordinates to  $iRC_3$  operations, there are 32 possible intermediates or transition states.<sup>28</sup> The explicit topological representation in polytopal form is *uniquely* the reduction (*cell first*) of the  $\gamma_4$  regular polytope (tesseract) into three dimensions (Figure 7). Unique reaction paths traversing the outside and inside vertices comprise the eight Bailar<sup>21</sup> or Springer and Sievers<sup>24</sup> intermediates, and the remaining edges are Ráy and Dutt intermediates.<sup>22</sup> The minimum number of steps for enantiomer traverse is three and the process has sixfold degeneracy for the hypothetical  $M(\text{chel})_3$  case. The two isomer “subcycles” or circuits are four—all faces or polygons are tetragons. This figure becomes a potential energy surface by placing the energy origin at a point equidistant from the vertices of a trapezoidal cross section and by conversion of all straight line connectors (to vertices) to curves which are *outside* the tesseract. The loss of the isomer subcycle of three and the reduction of the enantiomer traverse degeneracy to six are due to the chelate restraints in  $RC_3$  operations (compared to the general  $ML_6$  case).

### Concluding Remarks

This discussion of octahedral intramolecular rearrangements has been presented in terms of an idealized  $RC_3$  or  $iRC_3$  face rotation (eq 1). Less symmetric or idealized mechanisms must be entertained in a thorough analysis (*vide infra*) although, at this stage, experimental distinctions among intramolecular processes do not appear feasible. In any case, the possibility of alternative intramolecular rearrangements does not impair the generality of the foregoing topological representations.

A distinction must be made in nomenclature, often employed today, between rearrangement mechanisms and intermediates or transition states. To date, two basic types of octahedral rearrangements have been proposed. One is the previously discussed face rota-

(27) A possible system worthy of experimental study is  $\text{Rh}(\text{CH}_3\text{-COCHCOCF}_3)(\text{CF}_3\text{COCHCOCH}_2\text{C}_6\text{H}_5)(\text{CH}_3\text{COCHCOCH}_2\text{C}_6\text{H}_5)$ .

(28) The notations are (l) octahedral: (1) -135, 246, (2) -153, 264, (3) -145, 236, (4) -163, 254, (5) -146, 235, (6) -164, 253, (7) -136, 245, (8) -154, 263; and (d) trigonal prism: (1) -135, 246, (2) -145, 236, (3) -136, 245, (4) -146, 235, (5) -143, 265, (6) -134, 265, (7) -243, 165, (8) -234, 165, (9) -312, 456, (10) -312, 465, (11) -412, 356, (12) -412, 365, (13) -512, 634, (14) -512, 643, (15) -612, 534, (16) -612, 543. The “d” forms of trigonal prisms in the order 1 through 16 are the intermediates for the following octahedral rearrangements:  $l_2-d_1$ ,  $l_3-d_3$ ,  $l_4-d_1$ ,  $l_5-d_5$ ,  $l_2-d_5$ ,  $l_3-d_3$ ,  $l_5-d_1$ ,  $l_1-d_3$ ,  $l_3-d_1$ ,  $l_5-d_1$ ,  $l_2-d_3$ ,  $l_1-d_5$ ,  $l_3-d_5$ ,  $l_5-d_3$ , and  $l_5-d_5$ , respectively.

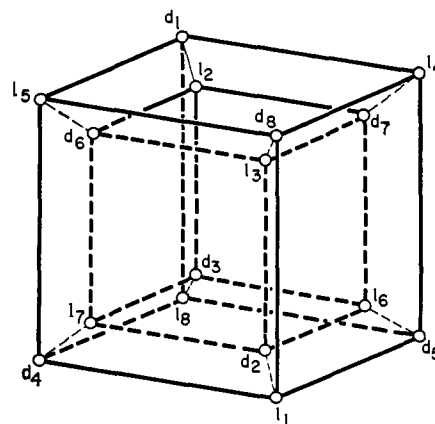


Figure 7. Topological representation of the general case for a six-coordinate tris-chelate system wherein all of the chelate ligand atoms are different. The topological figure is the cell first three-dimensional reduction of the tesseract which has 16 vertices representing the 16 octahedral stereoisomers. Trigonal prismatic intermediates are at the edge midpoints.<sup>28</sup> The eight diagonals connecting the outer and inner vertices involve “Bailar”-type intermediates and the remaining 24, trigonal prismatic stereoisomers of the “Ráy and Dutt” type. The three-dimensional projection of the tesseract *strictly* applies only to the hypothetical case  $M(\text{chel})_3$  in which all six chelate ligand atoms are identical but distinguishable by labeling (as per the  $ML_6$  case represented by the pentagonal dodecahedron in double group form). This is a dihedral group.

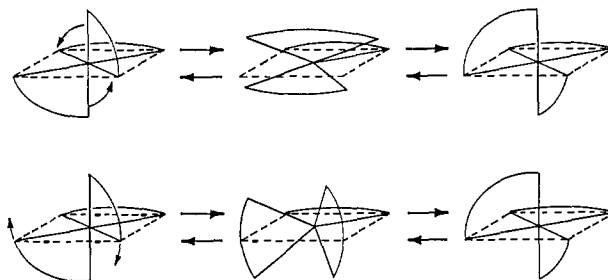


Figure 8. Depiction of the alternative mechanism to face rotation ( $iRC_3$ ) for rearrangement of octahedral complexes. The chelate rings remain essentially rigid and two are rotated in either of two directions. The top direction of rotation generates a “Bailar”-type intermediate and the bottom a “Ráy and Dutt”-type intermediate. These processes, depicted specifically for chelates, are generally applicable to all types of six-coordinate complexes.

tion,  $RC_3$  or  $iRC_3$  operation, which may be generically referred to as a Bailar Twist.<sup>21</sup> The second<sup>22,24</sup> comprises conversion of a diamond face of the octahedron to a square face and rotation of the square face relative to the opposite edge parallel to the inner edge of the initial diamond face. This is illustrated in Figure 8 for the specific case of tris chelates. Although a general mechanism, this process, depending upon the direction of rotation, can generate a near- $D_{3h}$ - or a  $C_{2v}$ -type intermediate, which rotations may be called Ráy–Dutt<sup>22</sup> or Springer–Sievers<sup>24</sup> processes. The two kinds of trigonal prismatic or near trigonal prismatic intermediates,  $D_{3h}$  and  $C_{2v}$ , are commonly referred to as Bailar<sup>21</sup> and as Ráy and Dutt,<sup>22</sup> respectively.

A final comment on stereochemical nonrigidity is in order. For any  $x$ -coordinate complex or molecular cluster, stereochemical lability stems from a variety of processes, including dissociation, association, solvation, and rearrangements comprising constitutional isomerism—all of which have some finite rate although in-

dividual rates *may* differ widely. Assay of dynamic processes with a single technique of severely limited time scale, especially a resonance probe, tends to limit the experimentalist's purview. Nuclear magnetic resonance studies may define a nonbond-breaking mechanism as the origin of stereochemical lability, but there may be a dissociative process, differing in rate by only  $10^2$ , contributing significantly to the general phenomenon.

Topological delineation of stereoisomeric processes is being developed for 3- through 12-atom aggregates. Solutions are being sought primarily in polytopes and toruses to maximize the possibility of facile progression to a potential energy surface. An initial paper, to be submitted shortly, will outline definitions,<sup>29</sup> constraints, and approaches to generic topological representations.

(29) *E. g.*, isomer numbers, connectivity, closed and open systems, subsystems, subcycles, and enantiomer traverse.

## Structural Studies of Pentacoordinate Silicon. II. Phenyl(2,2',2''-nitrilotriphenoxy)silane<sup>1</sup>

F. Peter Boer, June W. Turley, and John J. Flynn

*Contribution from the Dow Chemical Company, Eastern Research Laboratory, Wayland, Massachusetts 01778, and Chemical Physics Research Laboratory, Midland, Michigan 48640. Received March 26, 1968*

**Abstract:** The molecular and crystal structure of  $(C_6H_5)_3Si(OC_6H_4)_3N$  has been determined from three-dimensional X-ray diffraction data. The space group is  $Cmc2_1$  with four molecules in an orthorhombic unit cell of dimensions  $a = 11.229 \pm 0.003 \text{ \AA}$ ,  $b = 14.767 \pm 0.004 \text{ \AA}$ , and  $c = 11.940 \pm 0.003 \text{ \AA}$ . The molecules exhibit  $C_2$  symmetry, with the plane of the phenyl substituent oriented perpendicular to the crystallographic mirror plane. The main features of interest are the Si-N bond length of  $2.334 \text{ \AA}$ , which gives the first direct evidence for Si→N dative bonding in nitrilotriphenoxy silanes, and the C-Si-O bond angles of  $100.0^\circ$  (average), which indicate the geometry at silicon to be distorted slightly further from an ideal trigonal bipyramid than the analogous nitrilotriethoxysilane. Other bond distances at silicon are Si-C =  $1.853 \text{ \AA}$ , Si-O(1) =  $1.635 \text{ \AA}$ , and Si-O(2) =  $1.650 \text{ \AA}$ . The final discrepancy index  $R_1$  is 0.0599 for 858 reflections.

Recent X-ray diffraction studies of dimethylsilylamine pentamer,<sup>2</sup>  $(-SiH_3N(CH_3)_2)_5$ , and phenyl-nitrilotriethoxysilane,<sup>1</sup>  $PhSi(OCH_2CH_2)_3N$ , have directly established the existence of pentacoordinate silicon in solids. Similar bonding has also been hypothesized to occur in nitrilotriphenoxy silanes,<sup>3</sup>  $XSi(OC_6H_4)_3N$ . Until the present study, the principal evidence for this assertion was the absence of basicity in these compounds, particularly as compared to certain triaryl-amines such as azatriptycene, where the rings are constrained from aligning themselves so that their  $\pi$  orbitals can effectively delocalize the N lone-pair electrons. This lack of basicity is consistent with a transannular Si←N dative bond and also occurs in the nitrilotriethoxysilanes.<sup>4</sup> The present single-crystal X-ray diffraction study of phenyl-nitrilotriphenoxy silane, where  $X = C_6H_5$ , provides direct evidence for the existence of this bond and shows that the silicon coordination geometry is even further distorted from an ideal trigonal bipyramid in this structure than in phenyl-nitrilotriethoxysilane.

### Experimental Section

**Data Collection.** A single crystal, in the shape of a rough sphere of approximately 0.1 mm radius, was examined by photographic

methods to determine the space group and preliminary lattice constants, and then carefully centered on a Picker automatic four-circle diffractometer. Accurate lattice constants were obtained by a least-squares refinement of the setting angles of ten reflections with Cu  $K\alpha$  radiation ( $\lambda$  1.5418  $\text{\AA}$ ). The reciprocal lattice symmetry,  $D_{2h}$ , indicated that the crystal belonged to the orthorhombic system, with unit cell dimensions  $a = 11.229 \pm 0.003 \text{ \AA}$ ,  $b = 14.767 \pm 0.004 \text{ \AA}$ , and  $c = 11.940 \pm 0.003 \text{ \AA}$ , giving a calculated density  $\rho = 1.326 \text{ g cm}^{-3}$  for  $Z = 4$ . The reflection conditions ( $hkl$ ,  $h + k = 2n$ ; and  $h0l$ ,  $h = 2n$ ,  $l = 2n$ ) were consistent with space groups  $Cmc2_1$ ,  $C2cm$ , and  $Cmcm$ . Although  $Cmcm$  was considered unreasonable because it required either  $C_{2h}$  or  $C_{2v}$  molecular symmetry, a final choice between the remaining two space groups could not be made until the structure was determined.

The intensity data were collected using the  $2\theta$  scan mode of the diffractometer with Ni-filtered Cu  $K\alpha$  radiation. The X-ray tube was set at a  $3^\circ$  take-off angle, and a detector aperture 4.0 mm square was placed 30 cm from the crystal. Scan angles from  $1.9$  to  $2.5^\circ$  were employed over the range ( $0$ – $130^\circ$ ) of  $2\theta$  examined. The scan speed was  $2^\circ/\text{min}$ . Background counts of 15 sec were taken at each end of the scan by the stationary-crystal-stationary-counter technique. A data set comprising 891 of the 1249 possible reflections in the Cu  $K\alpha$  sphere was observed. The intensities of 28 of these reflections were, however, judged to be too weak to be statistically significant and were omitted from the structure analysis. For the remainder, an error  $\sigma(I) = [(0.05I)^2 + N_0 + k^2N_b]^{1/2}$  was assigned to the net intensity  $I = N_0 - kN_b$  in order to establish the weights  $w = 4F^2/\sigma^2(F^2)$  for subsequent least-squares refinement. Here  $N_0$  is the gross count,  $N_b$  is the background count, and  $k$  is the ratio of scan time to background time. The data were then corrected for Lorentz and polarization effects and an absolute scale factor and over-all temperature factor were computed by Wilson's method. No absorption corrections were made in view of the low linear absorption coefficient,  $\mu(\text{Cu } K\alpha) = 12.1 \text{ cm}^{-1}$ , and the relatively small crystal size.

**Structure Determination and Refinement.** A three-dimensional sharpened Patterson function was computed.<sup>5a</sup> While the Patter-

(1) Paper I: J. W. Turley and F. P. Boer, *J. Am. Chem. Soc.*, **90**, 4026 (1968).

(2) R. Rudman, W. C. Hamilton, S. Novick, and T. D. Goldfarb, *ibid.*, **89**, 5157 (1967).

(3) C. L. Frye, G. A. Vincent, and G. L. Hauschildt, *ibid.*, **88**, 2727 (1966).

(4) C. L. Frye, G. E. Vogel, and J. A. Hall, *ibid.*, **83**, 996 (1961).